Modelling of beams using the reduced integration technique: statics and free vibrations

M. Kekana* J. Badur†

Received May 1999; Final version November 1999

There has been considerable interest over the past two decades in studies of locking phenomenon that occurs in shell, plate and beam elements. This has largely been due to the misunderstanding of the role of reduced integration – on the modelling of the displacement field across the thickness. Therefore, the phenomenon of locking is reviewed and re-examined using, as an illustrative example, a model of thick and thin elastic beam.

It is shown that by introducing reduced integration in the stiffness matrix, instead of full integration, we introduce to the model an assumption that straight segment normal to the mid-surface before deformation stays normal after deformation. That is, reduced integration introduces the Kirchhoff-Love assumption at the numerical level. Appropriate calculations regarding thick and thin beams are presented and discussed.

Nomenclature

A	area
E	elastic moduli
G	rigidity moduli
I	moment of inertia
H	functional
$\mathcal{L}$	Lagrangian
N_i	interpolation functions
b	width
h	height
j	number of nodes in an element
k	shear correction facttor
q	uniformly distributed load
t, t_0	time variable, constant
$\tilde{v}_i$	discrete displacement field
w	deflection in z-axis
(u_x, u_y, u_z)	continuous displacement field
(x, y, z)	Cartesian co-ordinates
Φ	vector of mode shapes
ω	frequency of vibration
δ	small increment operator
ρ	material density
θ	rotation
ε_{xx}	normal strains
γ_{xz}	shear strains
σ_{xx}	normal stress
τ_{xz}	shear stress

Introduction

Vibrations in most machines, structures and dynamic systems are undesirable because of the resulting unpleasant motions, noise and dynamic stresses which may lead to fatigue and failure of the structure or machine. In addition, it causes energy dissipation and reduction in the overall performance of the structure or machine. Therefore, it is essential to analyse the vibration of structures by predicting the natural frequencies and the response expected in the event of an excitation. Natural frequencies are important considering that when the frequency of the disturbing force coincides with the natural frequency resonance occurs. At this state, the amplitude of vibration increases indefinitely as well as the dynamic stresses and noise levels; making it desirable to control this excessive vibration and to effectively stabilise the structure after any disturbance. Using piezoelectric material for active sensing and control has drawn much attention recently. Chandrashekhara,[5] Salemi,[6] Lesieutre[7] and others have studied applications of piezoelectric material to active control of composite structures. However, at the numerical level, the effects of full and reduced integration schemes on the numerical solutions were not highlighted. Also, the effects of increasing number of elements in the simulation process were omitted.

In this paper, the Hamilton's principle will be used to develop the dynamic linear response of thin as well as thick beams. The static behaviour of the beam will be achieved by omitting the dynamic terms in the formulation. The effects of full and reduced integration schemes will be studied as well.

*Centre for Advanced Materials, Design and Prototyping Research, Technikon Natal, P.O. Box 953, Durban, 4000 South Africa
†Professor, IFFM Polish Academy of Sciences, Gdañsk

It is well known that the numerical solution obtained by increasing the number of finite elements approaches the analytical solution but it is not mentioned in the literature whether this condition holds indefinitely or not. Therefore, the effects of increasing the number of elements in the numerical solution will be investigated too.

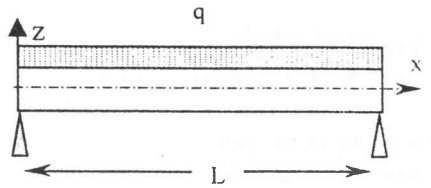

Figure 1 Simply supported beam subjected to uniformly distributed load q

Physical model

Consider a beam of rectangular cross-section as shown in Figure 1. The loading $q(x)$ is applied in the xy-plane and is directed transversely to the beam (such loading might include point loads and/or couples). The requirement is to determine static and dynamic behaviour or the beam under such loading.(1)

Displacement model

Usually, in the beam and shell theory it is assumed that normal fibres to the neutral axis before deformation remain straight and normal to the neutral axis after deformation. Indeed, if one took trouble to paint a straight line representing the normal on the side of an unloaded beam, the line would remain straight and normal after the beam is loaded as shown, in Figure 2, by a solid line.[3] This would not be true for a thick beam. The normal would take up the shape indicated, in Figure 2, by a broken line. Thus as a result of bending, a line segment dx in the undeformed geometry translates in the z-direction an amount $w(x)$ and, in addition, rotates in the $x-z$ plane an amount given by $\theta = w_{,x} + \phi$. In summary, the assumed displacement field for small deformation is given[2] as

$$\mathbf{u}(x,y,z,t) = \left\{ \begin{array}{c} u_x(x,y,z,t) \\ u_y(x,y,z,t) \\ u_z(x,y,z,t) \end{array} \right\} = \left\{ \begin{array}{c} z\theta(x,t) \\ 0 \\ -w(x,t) \end{array} \right\} \tag{1}$$

(1) Subject to $E = 70\text{GPa}$, $\rho = 2710\text{kg/m}^3$, $v = 0.25$, $\mathcal{L} = 0.4572$ m, width $(b) = 0.0254$ m, thickness $(h) = 0.008$ m, $q = 1$ N/m.

Strain model

The strains are defined in terms of the above displacement field by the expression

$$\varepsilon = \left\{ \begin{array}{c} \varepsilon_{xx} \\ \gamma_{xz} \end{array} \right\} = \left\{ \begin{array}{c} u_{x,x} \\ u_{x,z} + u_{z,x} \end{array} \right\} = \left\{ \begin{array}{c} z\theta_{,x} \\ \theta - w_{,x} \end{array} \right\} \tag{2}$$

Constitutive model

In this model, linear elastic behaviour of the material will be adopted wherein each stress component is simply related to the strains as in Hooke's law. That is[2]

$$\sigma = \left\{ \begin{array}{c} \sigma_{xx} \\ \tau_{xz} \end{array} \right\} = \left[\begin{array}{cc} E & 0 \\ 0 & kG \end{array} \right] \left\{ \begin{array}{c} \varepsilon_{xx} \\ \gamma_{xz} \end{array} \right\} \tag{3}$$

Energy approach

The kinetic energy (T) is expressed as

$$\begin{aligned} T &= \tfrac{1}{2} \int_{-h/2}^{h/2} \int_{-b/2}^{b/2} \int_{0}^{\mathcal{L}} \rho \left(\dot{\mathbf{u}}\right)^2 dxdydz \\ &= \tfrac{1}{2} \int_{0}^{\mathcal{L}} \left(\rho I \dot{\theta}^2 + \rho A \dot{w}^2 \right) dx \end{aligned} \tag{4}$$

where

$$\int_{-h/2}^{h/2} \int_{-b/2}^{b/2} \left\{ \begin{array}{c} z^2 \\ 1 \end{array} \right\} dydz = \left\{ \begin{array}{c} bh^3/12 \\ bh \end{array} \right\} = \left\{ \begin{array}{c} I \\ A \end{array} \right\}$$

The kinetic energy is thus composed of two parts. The first represent the kinetic energy due to rotation of beam elements, i.e. rotary inertia. For problems involving thin beams, rotation contribution of T may be neglected since its contribution is very small for long slender beams. The second represents the kinetic energy due to translatory motion in the vertical direction z.

Similarly, for very thin beams only the strain energy which is due to bending will be considered; this means that the energy due to stretching will be omitted. The strain energy (U) is expressed as

$$\begin{aligned} U &= \tfrac{1}{2} \int_{-h/2}^{h/2} \int_{-b/2}^{b/2} \int_{0}^{\mathcal{L}} \varepsilon^T \cdot \sigma \, dxdydz \\ &= \tfrac{1}{2} \int_{-h/2}^{h/2} \int_{-b/2}^{b/2} \int_{0}^{\mathcal{L}} \{\varepsilon_{xx} \; \gamma_{xz}\} \cdot \left\{ \begin{array}{c} \sigma_{xx} \\ \tau_{xz} \end{array} \right\} dxdydz \\ &= \tfrac{1}{2} \int_{0}^{\mathcal{L}} \left(EI\theta_{,x}^2 + kGA\left(\theta - w_{,x}\right)^2 \right) dx \end{aligned} \tag{5}$$

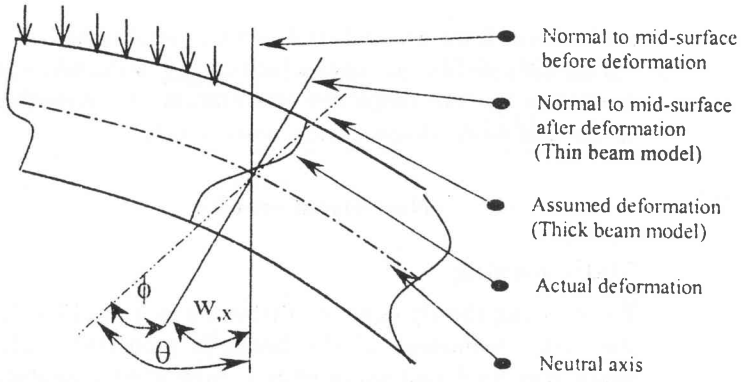

Figure 2 Cross-sectional deformation of a beam

Whereas, the external work done (V) is expressed as

$$V = \int_0^{\mathcal{L}} qwdx \tag{6}$$

Hamilton's variational model

For dynamics of the given beam, Hamilton's principle will be used to obtain, from all admissible paths that the beam can take from the undeformed configuration to the deformed configuration, the path that extremises the time integral of the total energy (Lagrangian) during the time interval. Hamilton's principle is expressed as

$$H(u_1,u_3) = \delta \int_{t_1}^{t_2} \mathcal{L}dt = \delta \int_{t_1}^{t_2} (T - U + V)\, dt = 0 \tag{7}$$

Substitution of (4), (5) and (6) into (7) yields

$$\begin{aligned} &\delta \int_{t_1}^{t_2}\int_0^{\mathcal{L}} \left(\tfrac{1}{2}\left(\rho I\dot{\theta}^2 + \rho A\dot{w}^2\right)\right. \\ &\left. -\tfrac{1}{2}\left(EI\theta_{,x}^2 + kGA\left(\theta - w_{,x}\right)^2\right) + qw\right) dxdt = 0 \end{aligned} \tag{8}$$

The extremisation of the flinctional $H(u_1,u_3)$ is carried out using the variational principle, in operator approach, given by

$$\int_x \delta\mathcal{L}(\theta,w)\, dx = \int_x \left(\frac{\partial\mathcal{L}}{\partial\theta}\delta\theta + \frac{\partial\mathcal{L}}{\partial w}\delta w\right) dx \tag{9}$$

In view of eqn (9), eqn (8) becomes

$$\begin{aligned} H = \int_{t_1}^{t_2}\int_0^{\mathcal{L}} &\left\{\delta\left(\dot{\theta}\right)\rho I\dot{\theta} + \delta\dot{w}\rho A\dot{w} - \delta\left(\theta_{,x}\right)EI\theta_{,x}\right. \\ &\left. -\delta\left(\theta - w_{,x}\right)kGA\left(\theta - w_{,x}\right) + q\delta w\right\} dxdt \end{aligned} \tag{10}$$

Finite element model

The aim now is to construct a finite element approximation of equation (10). Using the finite element method, the domain is discretised into non-overlapping finite elements. The solution, within an element,[1] is approximated as

$$\mathbf{v} = \sum_{i=1}^{j} N_i(x)\,\tilde{v}_i(t) = \mathbf{N}\tilde{\mathbf{v}} \tag{11}$$

Substituting (11) into (10) yields,

$$\begin{aligned} \int_{t_1}^{t_2}\int_0^{\mathcal{L}} &\left(\delta\left(\mathbf{N}\dot{\tilde{\theta}}\right)^T \rho I\mathbf{N}\dot{\tilde{\theta}} + \delta\left(\mathbf{N}\dot{\tilde{\mathbf{w}}}\right)^T \rho A\mathbf{N}\dot{\tilde{\mathbf{w}}}\right. \\ &-\delta\left(\mathbf{N}\tilde{\theta} - (\mathbf{N}\tilde{\mathbf{w}})_{,x}\right)^T kGA\left(\mathbf{N}\tilde{\theta} - (\mathbf{N}\tilde{\mathbf{w}})_{,x}\right) \\ &\left.-\delta\left(\mathbf{N}\tilde{\theta}\right)_{,x}^T EI\left(\mathbf{N}\tilde{\theta}\right)_{,x} + q\delta(\mathbf{N}\tilde{\mathbf{w}})\right) dxdt = 0 \end{aligned} \tag{12}$$

Eqn (12) is simplified by taking its first variation; integrating by parts, regrouping terms and observing that

$$\delta\theta\,|_{t_1}^{t_2} = \delta w|_{t_1}^{t_2} = 0$$

would lead to trivial solutions. Granted that ρ, k, A, E, I and G are constants, this gives the governing equations describing the motion of a beam, in finite element form, as

$$\begin{aligned} &\int_{t_1}^{t_2}\int_0^{\mathcal{L}} \left\{\begin{array}{l} -\frac{\partial}{\partial t}\left(\mathbf{N}^T\rho A\mathbf{N}\dot{\tilde{\mathbf{w}}}\right) + \frac{\partial}{\partial x} \\ \times\left(\mathbf{N}^T kGA\left((\mathbf{N}\tilde{\mathbf{w}})_{,x} - \mathbf{N}\tilde{\theta}\right)\right) + \mathbf{N}^T q \end{array}\right\} \\ &\times dxdt = 0 \end{aligned}$$

$$\begin{aligned} &\int_{t_1}^{t_2}\int_0^{\mathcal{L}} \left\{\begin{array}{l} -\frac{\partial}{\partial t}\left(\mathbf{N}^T\rho I\mathbf{N}\dot{\tilde{\theta}}\right) + \frac{\partial}{\partial x}\left(\mathbf{N}^T EI\left(\mathbf{N}\tilde{\theta}\right)_{,x}\right) \\ +\mathbf{N}^T kGA\left((\mathbf{N}\tilde{\mathbf{w}})_{,x} - \mathbf{N}\tilde{\theta}\right) \end{array}\right\} \\ &\times dxdt = 0 \end{aligned} \tag{13}$$

Subject to boundary conditions

$$-\int_{t_1}^{t_2} \delta\tilde{\theta}^T \mathbf{N}^T EI \left(\mathbf{N}\tilde{\theta}\right)_{,x} \Big|_{x_1}^{x_2} dt$$

$$-\int_{t_1}^{t_2} \delta\tilde{\mathbf{w}}^T \mathbf{N}^T kGA \left((\mathbf{N}\tilde{\mathbf{w}})_{,x} - \mathbf{N}\tilde{\theta}\right) \Big|_{x_1}^{x_2} dt = 0 \quad (14)$$

and initial conditions

$$\int_0^{\mathcal{L}} \delta\tilde{\theta}^T \mathbf{N}^T \rho I \mathbf{N} \dot{\tilde{\theta}} \Big|_{t_1}^{t_2} dx$$

$$+\int_0^{\mathcal{L}} \delta\tilde{\mathbf{w}}^T \mathbf{N}^T \rho A \mathbf{N} \dot{\tilde{\mathbf{w}}} \Big|_{t_1}^{t_2} dx = 0 \quad (15)$$

Eqn (13) is written in matrix form as

$$\int_{t_1}^{t_2}\int_0^{\mathcal{L}} \left(\begin{bmatrix} N_i & 0 \\ 0 & N_i \end{bmatrix} \begin{bmatrix} \rho A & 0 \\ o & \rho I \end{bmatrix} \begin{bmatrix} N_i & 0 \\ 0 & N_i \end{bmatrix} \times \begin{Bmatrix} \ddot{\tilde{w}}_i \\ \ddot{\tilde{\theta}}_i \end{Bmatrix} + \begin{bmatrix} 0 & -N_{i,x} \\ N_{i,x} & N_i \end{bmatrix} \times \begin{bmatrix} EI & 0 \\ 0 & kGA \end{bmatrix} \begin{bmatrix} 0 & N_{i,x} \\ -N_{i,x} & N_i \end{bmatrix} \times \begin{Bmatrix} \tilde{w}_i \\ \tilde{\theta}_i \end{Bmatrix} - \begin{Bmatrix} N_i \\ 0 \end{Bmatrix} q \right) \times dx dt = 0 \quad (16)$$

or shortly as

$$\int_{t_1}^{t_2}\int_0^{\mathcal{L}} \left\{ \mathbf{N}^T \overline{\rho} \mathbf{N} \ddot{\tilde{\mathbf{v}}} + \mathbf{B}^T \mathbf{D} \mathbf{B} \tilde{\mathbf{v}} - \overline{\mathbf{N}}^T q \right\} dx dt$$

$$= \mathbf{M}\ddot{\tilde{\mathbf{v}}} + \mathbf{K}\tilde{\mathbf{v}} - \tilde{\mathbf{F}} = \mathbf{0} \quad (17)$$

Eigenproblem

Considering eqn (17), by setting $\tilde{\mathbf{F}} = \mathbf{0}$ the free vibration equations are re-written here as

$$\mathbf{M}\ddot{\tilde{\mathbf{v}}} + \mathbf{K}\tilde{\mathbf{v}} = \mathbf{0} \quad (18)$$

For these set of equations, the harmonic solutions of the form

$$\tilde{\mathbf{v}} = \Phi \sin\omega (t - t_0) \quad (19)$$

are assumed.[4] Substituting (19) into (18), the generalised eigenproblem

$$\mathbf{K}\Phi = \omega^2 \mathbf{M}\Phi \quad (20)$$

is obtained, from which Φ and ω must be obtained.

Eqn (20) yields the eigensolutions (ω_k^2, Φ_k), where k represents the kth frequency of vibration corresponding to the kth mode shape vector, respectively.

Numerical results

Static loading

By omitting the dynamic contribution in eqn (13–17), the static behaviour of the beam is modelled. The beam was modelled using simply supported boundary conditions and material data given in Figure 1. Results showing the deflection curve were generated from an in-house program. The deflections were obtained using one-dimensional three-noded elements, with full (3-Gauss points) and reduced (2-Gauss points) integration schemes.

The results obtained using full integration scheme underestimated the deflections of the beam relative to the analytical solution. This shows that full integration introduced fictitious stiffness into the beam. This made the beam appear stiffer. Such phenomenon is attributed to locking. For the current beam aspect ratio, that is $^h/_{\mathcal{L}} = {}^1/_{57.1}$, this fictitious stiffness is not necessary.

For reduced integration, results compared favourably with analytical results (see Table 1). From the physical point of view, reduced integration modified the assumed displacement field in eqn (1) at the numerical level. It introduced the assumption that a straight segment normal to the neutral axis before deformation stays normal and straight after deformation. Of course, looking at the beam aspect ratio of $^h/_{\mathcal{L}} = {}^1/_{57.1}$ qualifies this assumption.

For the beam aspect ratios $^1/_{100} \leq {}^h/_{\mathcal{L}} \leq 1$ the following were observed. As the beam aspect ratio $^h/_{\mathcal{L}} \rightarrow {}^1/_{10}$ full integration scheme modelled the deflection curve favourably compared to reduced integration (see Table 2). For the case where $^h/_{\mathcal{L}} \rightarrow 1$ both schemes produced results which were three-times more when compared to the analytical results, which meant that three-dimensional effects dominated on both numerical and analytical approaches. Bending moment and shear force results, shown in Appendix Figure A1 and Figure A2, were generated using reduced integration and four (4) elements. The FEM results compared favourably with the analytical results. The results presented were evaluated at integration points since better results are obtained there when compared to the nodal points. A bar graph was used since, in the FEM displacement method, the stresses are discontinuous between elements. For this reason, a trend-line has been included to show the graph that will be obtained when using the analytical method.

Table 1 Deflection results of a simply supported beam, h/L = 1/57.1

x-coord. [m]	FEM				Analytical [m× 10^{-6}]	
	2-elements [m× 10^{-6}]		4-elements [m× 10^{-6}]			
	3-Gauss points	2-Gauss points	3-Gauss points	2-Gauss points	Thick beam	Thin beam
0.0	0.0	0.0	0.0	0.0	0.0	0.0
0.1143	−4.5175	−5.2539	−5.0857	−5.3477	−5.3477	−5.3435
0.2286	−6.0323	−7.5052	−7.1559	−7.5052	−7.5052	−7.4997
0.3429	−4.5175	−5.2539	−5.0857	−5.3477	−5.3477	−5.3435
0.4572	0.0	0.0	0.0	0.0	0.0	0.0

Table 2 Maximum deflections at different aspect ratios

		FEM		Analytical [m× 10^{-6}]	
		4-elements [m× 10^{-6}]			
	Aspect ratio	3-Gauss points	2-Gauss points	Thick beam	Thin beam
Thin beam	$h=L/100$	38.226	40.188	40.208	40.179
	$h=L/50$	4.7980	5.0271	5.0260	5.0223
	$h=L/30$	1.0449	1.0877	1.0856	1.0848
	$h=L/20$	0.3133	0.3234	0.3217	0.3213
	$h=L/18$	0.2293	0.2361	0.2345	0.2343
	$h=L/16$	0.1619	0.1661	0.1647	0.1646
Thick beam	$h=L/14$	0.1091	0.1116	0.1103	0.1102
	$h=L/12$	0.0693	0.0706	0.0695	0.0694
	$h=L/10$	0.04056	0.04114	0.04021	0.04018
3-D effects	$h=L/1$	0.00013660	0.00013661	0.00004021	0.00004018

Table 3 Natural frequencies of a simply supported beam, h/L = 1/57.1

	FEM [2-Gauss points]		Analytical		FEM [3-Gauss points]	
ω_n^2	2-elements	4-elements	Thick beam[1]	Thin beam[1]	2-elements	4-elements
ω_1^2	3.134×10^5	3.073×10^5	3.068×10^5	3.071×10^5	3.765×10^5	3.219×10^5
ω_2^2	6.025×10^6	5.006×10^6	4.894×10^6	4.914×10^6	6.025×10^6	5.943×10^6
ω_3^2	9.118×10^7	2.731×10^7	2.465×10^7	2.487×10^7	2.368×10^9	3.723×10^7
ω_4^2	2.966×10^{10}	9.508×10^7	7.738×10^7	7.862×10^7	1.614×10^{12}	9.508×10^7

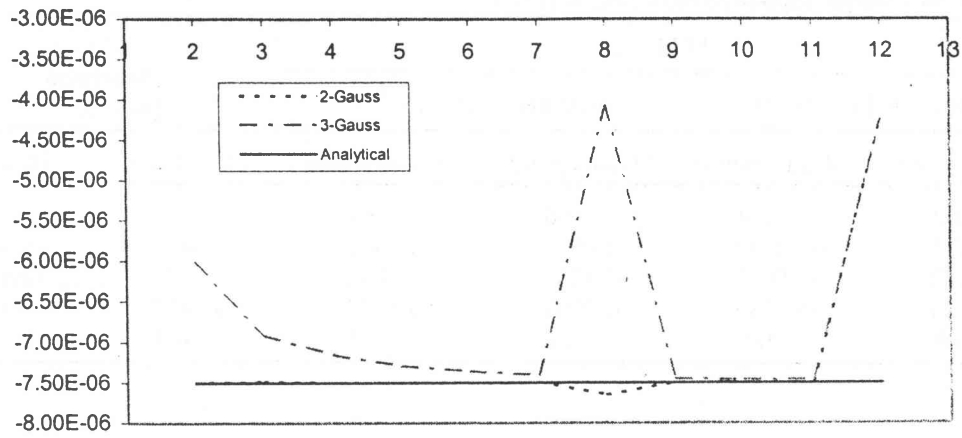

Figure 3 Maximum deflection versus number of elements

It is noted here, also, that convergence was observed with the increase in the number of elements. Furthermore, it was observed that when increasing the number of elements, that is when $h/\mathcal{L}_{\text{element}} \sim 1/10$, full integration scheme converged to the analytical value of displacements for thick and thin beam (see Figure 3), whereafter three-dimensional effects become dominant in both full and reduced integration.

Eigenproblem

The eigensolutions in eqn (20) were generated using the finite element stiffness and mass matrices. The boundary conditions were enforced by introducing, in the stiffness matrix, a large value on the corresponding diagonal of the nodes with prescribed displacemerts.

The natural frequencies, for the beam in Figure 1, are presented in Table 3 and the mode shapes, where full integration was employed on the mass matrix with reduced integration on the stiffness matrix, are shown in Figure A3 and Figure A4. It is noted that the fundamental frequency is pronounced when using full integration as compared to the other approaches presented here. This phenomenon is accredited to the fictitious stiffness introduced by full integration, since the stiffness has direct contribution to the frequency. That is, the stiffer the beam the higher the frequency.

Observing reduced integration results, a deviation from analytical results is observed for the second and higher frequencies. This deviation becomes pronounced at higher frequencies. This is accredited to the fewer elements used in the calculation of frequencies. To obtain results that are closer to the analytical solution, it is appropriate to use more elements.

Conclusion

In this paper, the dynamic system equations were developed using Hamilton's principle. By omitting the dynamic terms in the system of governing equations, the static behaviour was modelled. The effects of full and reduced integration schemes, in the stiffness matrix, were investigated in statics and free vibrations; the outcome of which provided a simple explanation of the locking phenomenon, from the numerical point of view. Currently, no meaningful results were obtained using reduced integration scheme on the mass matrix. However, these effects are under investigation. It was also observed that not only the beam aspect ratio played an important role in choosing a proper integration scheme but the element aspect ratio did too. Therefore, in the modelling of statics and free vibration of structures using the assumed displacement field, the choice of integration scheme and element density requires careful consideration.

Acknowledgements

The overall project has been funded by the Smart Composite Structures (NRF GUN: 2038139) and Peninsula Technikon. Their financial assistance is appreciated. The encouragement by Dr Bohua Sun is gratefully acknowledged.

References

1. Bathe K. *Finite element procedures.* Prentice Hall, 1996.

2. Dym CL & Shames IH. *Solid Mechanics.* McGraw-Hill.

3. Hinton E & Owen DJR. *Finite element programming.* Academic Press Inc., 1977.

4. Weaver W, Timoshenko SP & Young DH. *Vibration problems in engineering.* John Wiley & Sons, 1990.

5. Chandrashekhara K and Donthireddy P. Vibration suppression of composite beams with piezoelectric devices using a higher order theory. *Eur. J. Mech., A/Solids*, 1997, 16, pp.709–721.

6. Salemi P & Golnaraghi MF. Active control of forced and unforced structural vibration. *Journal of Sound and Vibration*, 1997, 208, pp.15–32.

7. Lesieutre GA & Lee U. A finite element for beams having segmented active constrained layers with frequency-dependent viscoelastics. *Smart Mater. Struct.*, 1996, 5, pp.615–627.

Appendix

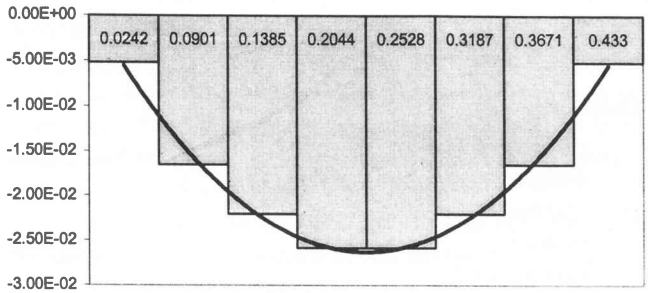

Figure A1 Bending moment diagram evaluated at Gauss points

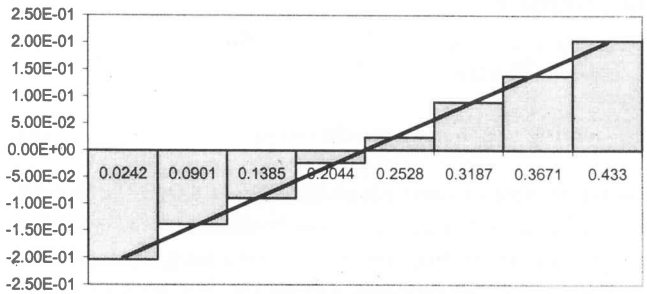

Figure A2 Shear force diagram evaluated at Gauss points

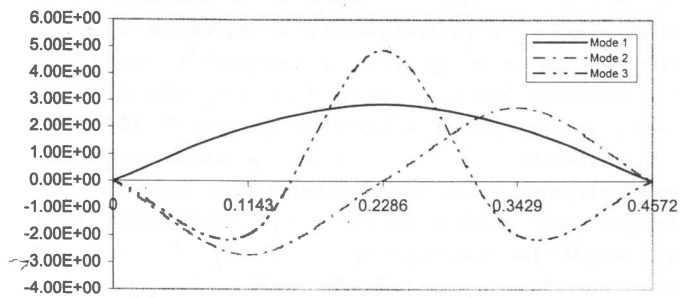

Figure A3 First three modes of free vibration using two elements

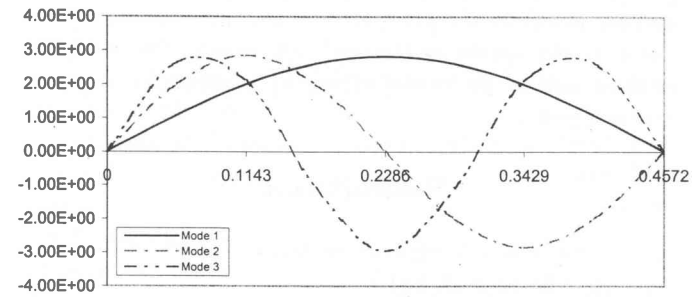

Figure A4 First three modes of free vibration using four elements